AMERICAN ACADEMY OF OPHTHALMOLOGY®

Delineating Corneal Elastic Anisotropy in a Porcine Model Using Noncontact OCT Elastography and Ex Vivo Mechanical Tests

Mitchell A. Kirby, PhD,[1] *John J. Pitre, Jr., PhD,*[1] *Hong-Cin Liou, PhD,*[1] *David S. Li, PhD,*[1] *Ruikang K. Wang, PhD,*[1,2] *Ivan Pelivanov, PhD,*[1] *Matthew O'Donnell, PhD,*[1] *Tueng T. Shen, MD, PhD*[1,2]

Purpose: To compare noncontact acoustic microtapping (AμT) OCT elastography (OCE) with destructive mechanical tests to confirm corneal elastic anisotropy.

Design: Ex vivo laboratory study with noncontact AμT-OCE followed by mechanical rheometry and extensometry.

Participants: Inflated cornea of whole-globe porcine eyes (n = 9).

Methods: A noncontact AμT transducer was used to launch propagating mechanical waves in the cornea that were imaged with phase-sensitive OCT at physiologically relevant controlled pressures. Reconstruction of both Young's modulus (*E*) and out-of-plane shear modulus (*G*) in the cornea from experimental data was performed using a nearly incompressible transversely isotropic (NITI) medium material model assuming spatial isotropy of corneal tensile properties. Corneal samples were excised and parallel plate rheometry was performed to measure shear modulus, *G*. Corneal samples were then subjected to strip extensometry to measure the Young's modulus, *E*.

Main Outcome Measures: Strong corneal anisotropy was confirmed with both AμT-OCE and mechanical tests, with the Young's (*E*) and shear (*G*) moduli differing by more than an order of magnitude. These results show that AμT-OCE can quantify both moduli simultaneously with a noncontact, noninvasive, clinically translatable technique.

Results: Mean of the OCE measured moduli were $E = 12 \pm 5$ MPa and $G = 31 \pm 11$ kPa at 5 mmHg and $E = 20 \pm 9$ MPa and $G = 61 \pm 29$ kPa at 20 mmHg. Tensile testing yielded a mean Young's modulus of 1 MPa − 20 MPa over a strain range of 1% to 7%. Shear storage and loss modulus (G′/G″) measured with rheometry was approximately 82/13 ± 12/4 kPa at 0.2 Hz and 133/29 ± 16/3 kPa at 16 Hz (0.1% strain).

Conclusions: The cornea is confirmed to be a strongly anisotropic elastic material that cannot be characterized with a single elastic modulus. The NITI model is the simplest one that accounts for the cornea's incompressibility and in-plane distribution of lamellae. AμT-OCE has been shown to be the only reported noncontact, noninvasive method to measure both elastic moduli. Submillimeter spatial resolution and near real-time operation can be achieved. Quantifying corneal elasticity in vivo will enable significant innovation in ophthalmology, helping to develop personalized biomechanical models of the eye that can predict response to ophthalmic interventions. *Ophthalmology Science 2021;1:100058* © *2021 by the American Academy of Ophthalmology. This is an open access article under the CC BY-NC-ND license (http://creativecommons.org/licenses/by-nc-nd/4.0/).*

Supplemental material available at www.ophthalmologyscience.org.

The cornea is one of the primary determinants of visual performance. Its structure of collagen fibrils embedded in a hydrated proteoglycan matrix forms a clear refractive component of the eye.[1,2] If corneal shape is not optimal, then images formed on the retina are aberrated. Many methods assess corneal shape, but no clinical tools predict shape changes from interventions such as LASIK and collagen cross-linking therapies. Despite the overall success of these interventions over the last decades, outcomes remain unpredictable for an individual patient, and many procedures produce unexpected changes in visual acuity and can have additional side effects. To optimize outcomes, a personalized corneal biomechanical model based on quantitative maps of mechanical moduli and intraocular pressure (IOP)-induced changes in mechanical moduli is needed to predict final corneal shape.

Unfortunately, personalized biomechanical models have not been developed completely. Initial attempts have used technologies based on tonometry (e.g., the Ocular Response Analyzer and Dynamic Scheimpflug Analyzer) to estimate in vivo corneal mechanical properties as part of IOP measurements. Early results suggest that tonometry may be a screening tool for disease progression in common conditions related to elasticity, such as glaucoma and myopia.[3,4]

https://doi.org/10.1016/j.xops.2021.100058
ISSN 2666-9145/21

However, it cannot determine fundamental material parameters required for robust biomechanical models of corneal deformation. In particular, tonometry metrics depend on experimental conditions and often characterize deformation in response to a dynamic mechanical stimulus over a large region of the cornea and sclera. In addition, tonometry does not consider the highly nonlinear stress−strain relationship between corneal tissue and preload IOP, nor does it account for material anisotropy or variations in corneal thickness. Thus to date, no noninvasive tools can map corneal elasticity (accounting for its strong anisotropy) to provide the information needed for a personalized biomechanical model suitable for screening, surgical planning, and treatment monitoring.

Advances in the imaging speed and sensitivity of OCT helped to launch OCT elastography (OCE), a technique to measure elastic moduli in the cornea at various length scales.[5] Recent developments in dynamic OCE produced technologies for noncontact excitation of propagating mechanical waves in the cornea and appropriate mechanical models for moduli reconstruction. Indeed, acoustic microtapping (AμT), which uses air-coupled ultrasound, is very effective at launching broadband, submillimeter-wavelength mechanical waves in OCE. In addition, a nearly incompressible transversely isotropic (NITI) medium model describing corneal anisotropy has been used to estimate both in-plane and out-of-plane shear moduli in the cornea by tracking propagating wavefields.[6]

In a recent AμT-OCE ex vivo whole-globe study, we showed that the cornea is a highly anisotropic elastic material, with up to 3 orders of magnitude difference between the in-plane Young's modulus E (mainly determining its deformation and shape) and the out-of-plane shear modulus G (mainly responsible for out-of-plane shearing).[6] However, direct comparison between invasive mechanical tests and noncontact AμT-OCE, a necessary step in validating the method and helping to translate it into a clinical tool, was not performed.

In this article, we report noncontact AμT-OCE measurements of both elastic moduli in 9 inflated porcine corneas of freshly excised whole eye globes at physiologically relevant controlled pressures and directly compare these measurements with mechanical tests performed on the same corneas immediately after AμT-OCE measurements. Parallel plate rheometry was used to measure the cornea's out-of-plane shear modulus; whereas, to quantify the cornea's Young's modulus, tensile measurements were performed with an extensometer.

Methods

Porcine Cornea Samples

Nine (n = 9) porcine eyes were enucleated carefully from healthy adult animals (3−5 months of age; 36−75 kg) by a specialist immediately after euthanasia. All excess tissue was removed to expose the sclera, and the remaining whole globe was rinsed with an ocular hydrating solution (balanced saline solution [BSS]). Whole globes were placed in a mold containing a damp sterile cotton pad to stabilize samples and mimic in vivo boundary conditions. A 20-gauge needle connected to a bath filled with BSS was inserted through the temporal wall of the sclera to apply a controlled internal hydrostatic pressure (IOP). The IOP was controlled by raising and lowering the bath and was calibrated previously using porcine whole globes where an additional 20-gauge needle was inserted into the wall of the sclera and was attached to a digital hydrostatic pressure sensor. After calibration, only a single needle insertion was performed in all AμT-OCE experiments. Each sample was held at the corresponding pressure for 5 minutes before scanning, over which a single drop of BSS was applied to prevent corneal dehydration. Each sample was scanned at room temperature and imaging took no longer than 1 hour per sample.

After AμT-OCE, samples were removed from the imaging system. An incision was made approximately 2 mm from the limbus around the sclera to remove the cornea from the globe. The lens, iris, and ciliary body were removed carefully using tweezers. Corneal buttons were rinsed with BSS and then placed in a damped cloth and immediately transported for rheometry at room temperature. Rheometry measurements were repeated twice and took approximately 1 hour per sample. A drop of BSS was applied immediately after the scan to prevent dehydration before extension testing.

Each corneal button then was sectioned into strips approximately 6 mm wide along the long-axis of the cornea (consistent with the nasotemporal direction[7]), leaving approximately 2 mm of sclera on each end. The strips were transported for tensile testing in the same damp cloth and were tested at room temperature within 1 hour of rheometry. Tensile loading and unloading was repeated 4 times. All data were acquired within 6 hours of animal euthanasia. No patient-level consent or institutional review board approval were required. All research adhered to the tenets of the Declaration of Helsinki.

Acoustic Microtapping OCT Elastography

Inflated eyes were placed on a vertical translation stage and raised to the focal plane of the polarization-maintaining, phase-stable AμT-OCE system (detail provided in Supplemental Methods). A single AμT-OCE scan generated and tracked elastic waves using OCT operating in M-B mode. At the start of each M-B sequence, a trigger signal was sent to an air-coupled acoustic transducer providing a temporally and spatially focused acoustic push pulse to create a localized displacement (tens-of-nanometer in amplitude) at the cornea's surface (Fig 1A) and to launch a pulsed elastic wave propagating along the cornea's surface (Fig 1B). Five hundred twelve repeated OCT A-scans (referred to as an M-scan) were obtained a set distance from the AμT focus. The propagating elastic wave was tracked with OCT along the anterior corneal surface using a sequence of M-scans conducted at 256 spatial locations in the nasotemporal direction to form a 1.5 × 10-mm (axial × lateral) corneal scan (B-scan) for every time instant relative to the start of each sequence. The entire spatiotemporal scan took 1.33 seconds.

The AμT OCE system was tested first using isotropic phantoms to validate the performance with a simple mechanical model (detailed in Supplemental Methods). Cornea whole globes then were scanned, and a 2-dimensional Fourier transform was applied to measured wavefields. A solution to the dispersion relationship was found by varying the in-plane tensile and out-of-plane shear moduli to converge on a best-fit solution using an optimization routine applied to 2-dimensional spectra (frequency-wavenumber domain, detailed in Supplemental Methods). This approach iteratively converged on a quantitative estimate of both the in-plane shear modulus μ (which then can be converted to $E = 3\mu$ under the assumption of corneal tensile isotropy) and out-of-plane (G) shear moduli (Fig 1C). The corneal thickness (h) was

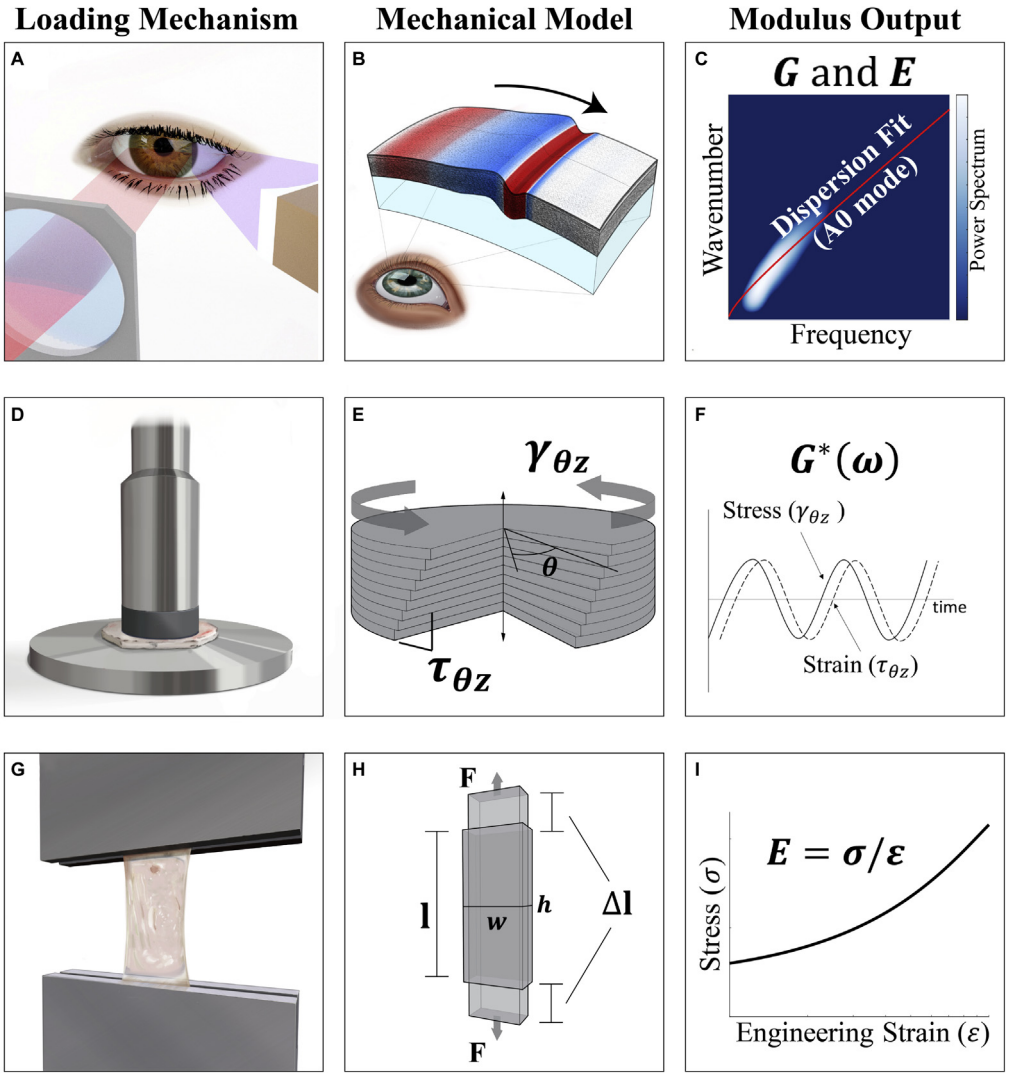

Figure 1. **A**, Representative display of an acoustic microtapping OCT elastography system to generate and image elastic waves in the cornea. The purple triangle represents noncontact acoustic loading through air and the red line-scan displays the approximate OCT scan range. **B**, Diagram showing guided elastic waves propagating in a nearly incompressible transversely isotropic material such as the cornea. **C**, Diagram showing that a solution to the dispersion equation was solved iteratively in the Fourier spectrum to reconstruct both elastic moduli, μ ($E = 3\mu$, under the assumption of corneal tensile isotropy) and G, that most closely resemble the measured waveform in the cornea. **D**, Representation of ex vivo parallel plate rheometry of the cornea. **E**, Material model demonstrating assumed geometries and shear stress-strain relationships. **F**, Calculation of the complex shear modulus G* using measured shear stress and strain. **G**, Representation of corneal strips loaded in an extensometer. **H**, Material model demonstrating assumed geometries and loading in tensile testing. **I**, Graph showing calculation of the Young's modulus, *E*, in extension testing.

determined using automated segmentation of the OCT image and served as a constraint on solutions to the dispersion relation.

Parallel Plate Rheometry

A parallel compression plate matching the approximate size of the cornea (12-mm diameter) clamped the anterior and posterior surfaces of the corneal buttons using a pneumatic rheometer (Anton Paar MCR 301 Physica; Fig 1D). A relative twisting force (sinusoidal oscillatory shear stress) about an axis perpendicular to the surface was applied under a 5 N compressive preload, and the resulting shear strain was measured to calculate the out-of-plane shear moduli, *G*, assuming a homogenous cylindrical material (Fig 1E, F, corresponding equations in "Results" and additional detail provided in Supplemental Methods).

Stress–Strain Extensometry

Each cornea was cut into a strip and pneumatically clamped (2752-005 BioPuls submersible pneumatic grips, 250 N max load) at the corneal–scleral boundary (Fig 1G). A 50-mN axial preload was applied and the samples were stretched at 2 mm/minute (Instron model 5543) up to 10% strain. For each sample, 2 load–unload cycles were performed to precondition the tissue, followed by 3 rounds of force-elongation followed by relaxation. The Young's modulus was determined assuming a beam-like structure (Fig 1H) and was defined by the tangential slope of the stress–strain curve (Fig 1I, corresponding equations in "Results" and additional detail provided in Supplemental Methods).

Results

Determination of Corneal Elastic Moduli with Acoustic Microtapping OCT Elastography

The cornea was modeled as a layer of a NITI material bounded by air on top and by water on bottom. As shown previously, the cornea can be treated as a flat NITI layer for wave propagation because its thickness is much smaller than its radius of curvature.[6] Consequently, guided waves propagating in the cornea exhibit a unique dispersion relationship defined in the NITI model by the Young's modulus $E = 3\mu$ (under the assumption of corneal tensile isotropy) and transverse shear modulus G (detailed in Supplemental Methods). The stress response to an induced strain for such a material is described using Hooke's law:

$$\begin{bmatrix} \sigma_{xx} \\ \sigma_{yy} \\ \sigma_{zz} \\ \tau_{yz} \\ \tau_{xz} \\ \tau_{xy} \end{bmatrix} = \begin{bmatrix} \lambda+2\mu & \lambda & \lambda & & & \\ \lambda & \lambda+2\mu & \lambda & & & \\ \lambda & \lambda & \lambda+2\mu & & & \\ & & & G & & \\ & & & & G & \\ & & & & & \mu \end{bmatrix} \begin{bmatrix} \varepsilon_{xx} \\ \varepsilon_{yy} \\ \varepsilon_{zz} \\ \gamma_{yz} \\ \gamma_{xz} \\ \gamma_{xy} \end{bmatrix} \quad (1)$$

where σ_{ij} denotes engineering stress, ε_{ij} denotes engineering strain, τ_{ij} denotes shear stresses, $\gamma_{ij} = 2\varepsilon_{ij}$ denotes shear strains, and the subscripts x, y, and z refer to standard Cartesian axes (a detailed description of elastic waves in NITI materials can be found in Pitre et al[6]). Note that in nearly incompressible media (such as all soft biological tissues) the longitudinal modulus λ does not influence medium deformation, although it is much larger than μ and G. Thus, functional biomechanical models do not require estimating λ.

The AμT-OCE system (see "Methods" and Supplemental Methods) was used to track propagating mechanical waves in porcine corneas. In all scans, wave energy was concentrated in a single dispersive wave mode (consistent with the A0-mode) and provided a reliable fit with the dispersion relationship for an NITI model. Measured wavefields were processed as described previously[6] to reconstruct both corneal moduli μ and G (Fig 1G).

Elastic moduli were reconstructed from OCE data for 9 corneas. On average (statistical mean), in-plane Young's modulus (E) was 12 ± 5 MPa at 5 mmHg and 20 ± 9 MPa at 20 mmHg. The mean transverse shear modulus (G) was 31 ± 11 kPa at 5 mmHg and 61 ± 29 kPa at 20 mmHg. The inflation pressure placed the cornea in a state of pre-stress, which varied in magnitude according to the IOP. This result demonstrated that both in-plane tensile and out-of-plane shear moduli increase with increasing IOP, consistent with the nonlinear material properties of the cornea. Note that both Young's and shear moduli changed by 98 ± 29% and 67 ± 15%, respectively, relative to the value measured at 5 mmHg as the pressure increased to 20 mmHg (see Supplemental Methods). The mean ± standard deviation of corneal thickness (assuming refractive index n = 1.389[8]) was 0.76 ± 0.10 mm at 5 mmHg and thinned on average by 50 μm as the pressure was increased. In all samples, the endothelium appeared intact.

Determination of the Out-of-Plane Shear Modulus with Parallel Plate Rheometry

Corresponding corneal buttons were deformed in a state of pure transverse shear strain according to:

$$\gamma_{\theta Z}(t) = \gamma_{\theta Z_0} e^{i\omega t} \quad (2)$$

where $i = \sqrt{-1}$, ω is the angular frequency, t is time, and $\gamma_{\theta z_0}$ is the peak shear strain amplitude. Collagen-rich tissue generally is linearly elastic at less than 1%[9]; thus, 0.1% peak shear strain was applied during the frequency sweep. The shear stress ($\tau\theta_z$) is described by:

$$\tau_{\theta z}(t) = \tau_{\theta z_0} e^{(i(\omega t+\theta))} \quad (3)$$

where $\tau_{\theta z_0}$ is the shear stress amplitude and θ is the phase shift angle between applied stress and the corresponding shear strain. The shear stress and strain relationships can be described by:

$$\tau_{\theta z}(t) = G^*(\omega)\gamma_{\theta z}(t) \quad 4$$

where the complex shear modulus, $G^*(\omega) = G'(\omega) + iG''(\omega)$ is defined by the in-phase (storage (G')) and out-of-phase (loss (G'')) stress-strain relationships. Frequency-dependent storage and loss moduli of the complex G value in the NITI model (detailed in Supplemental Methods) were determined over a range of 0.16 to 16 Hz. Sample thickness was recorded based on the parallel plate gap distance.

The shear storage and loss modulus G'/G'' measured in corresponding porcine corneal buttons subject to frequency-swept rotational shearing ranged from 82/13 ± 12/4 kPa to 133/29 ± 16/3 kPa for 0.16 to 16 Hz at 0.1% peak strain amplitude. Corneal buttons were tested using the smallest compressional preload that could be applied without tissue slippage and incorporated a portion of the scleral rim. The unconfined compression caused a portion of the tissue to splay beyond the custom-printed disk during testing. A single frequency sweep took approximately 30 minutes, over which each sample progressively thinned by approximately 27 μm. The mean value of the thickness was 0.80 ± 0.09 mm, averaged over the duration of each frequency sweep.

Determination of Corneal Young's Modulus with Stress–Strain Extensometry

The engineering stress and strain were calculated using the cross-sectional area of the cornea (measured with a digital micrometer) and force-elongation recordings assuming a beam structure (detailed in Supplemental Methods). In this configuration, the tissue was subject to uniaxial tension along the nasotemporal (xx) direction and the corresponding stress–strain relationship described by:

$$E = \frac{\sigma_{xx}}{\varepsilon_{xx}}, \quad (5)$$

where the strain-dependent Young's modulus was defined as the instantaneous slope of the stress–strain curve. The

tangential (Young's) modulus E measured in tensile testing over a range of engineering strain from 1% to 10% was 1.4 to 40 MPa (Supplemental Methods). The orientation of the strip lay in the xy-plane and the direction of the loading stress was uniaxial along the nasotemporal axis. The thickness of each sample was measured before extension testing in each sample. Corneal strips on average were 0.77 ± 0.09 mm thick and 5.9 ± 0.4 mm wide, resulting in a cross-sectional area of 4.6 mm^2.

It can be shown that for the xx-loading direction in an NITI material, E is sensitive only to the in-plane elastic modulus (detailed in Supplemental Methods). Based on this analysis, AμT-OCE provides a functionally equivalent measure of the elastic moduli probed in both shear rheometry (G) and tensile extension (E), but in a single, noncontact acquisition that can be performed noninvasively using intact whole-globe eyes.

Comparison between Methods

A direct comparison between the mean and standard deviation of the moduli measured via OCE, shear rheometry, and strip extensometry is shown in Figure 2. Most notably, both the tensile elastic modulus E and shear modulus G differ by approximately an order of magnitude, consistent with previous results.[6]

To compare OCE tests of inflated cornea with rheometry and extensometry, boundary conditions and equivalent strain effects were estimated. In rheometry, the scleral rim was retained to provide a surface to grip during tensile loading. To account for the effect of excess sclera, 3 separate cornea buttons were tested with the scleral ring and then immediately after removing the rim. The results (Fig 2; detailed in Supplemental Methods) indicate that the excess tissue induced an approximately 2-fold increase in the shear modulus compared with rheometry of the cornea alone. Consequently, a scaling factor was applied to rheometry results. Both the apparent (with sclera) and adjusted (without sclera) shear modulus range is displayed for comparison. Of note, the NITI model assumes a negligible viscosity. Thus, we compared the G value from OCE with the storage modulus (G') in rheometry.

Because the cornea inflated via IOP is under a state of tension, an estimated strain offset was introduced to account for tensile strain resulting from IOP as well as compressive forces within the anterior portion of the cornea produced when flattening a curved structure (detailed in Supplemental Methods) during elongation. The strain offset first references the state where strips were exposed only to tension, and then internal pressure (within the tissue) was used to predict equivalent strain values within the samples loaded via inflation and strip extension. At an IOP of 5 to 20 mmHg, the equivalent engineering tensile strain was estimated to be between $4.0 \pm 0.2\%$ and $5.8 \pm 0.9\%$. The Young's modulus estimate from OCE corresponded to an equivalent strain of between 5.8% and 7.0% in strip extensometry. In general, measurements obtained via different methods tracked each other, but were not highly correlated for the same samples.

Discussion

Predicting corneal shape changes after medical interventions and longitudinal alterations from postprocedure performance is critically important to improve screening, surgical planning, treatment monitoring, and overall outcomes in vision correction therapies. Because of the structural complexity and mechanical nonlinearity (i.e., IOP-dependent moduli) of the cornea, a personalized mechanical model is required to optimize procedure outcomes. Such a model must include in vivo measurements of topography, IOP, and maps of corneal mechanical moduli. Because the IOP is not consistent and the corneal elastic moduli are nonlinear, moduli changes induced by variations in IOP also must be considered. To date, reliable measurements of ocular mechanical properties have been possible only on ex vivo samples and have not impacted the clinic directly.[10] Although critical to our understanding of corneal mechanics, the destructive nature of most traditional techniques render these approaches impractical for clinical translation.

Anterior segment OCT can map corneal shape, and tonometry can estimate IOP. However, only recently a noncontact method has been shown to provide quantitative information on corneal elasticity. In a recent study, we showed that noncontact AμT-OCE can assess both corneal moduli, E and G, simultaneously under physiologic loading conditions.[6] It was very important that the AμT-OCE measured in-plane Young's modulus, E, was in good correspondence with literature results obtained by destructive ex vivo inflation and tensile tests, whereas the out-of-plane shear modulus G, being a few orders of magnitude smaller than E, reasonably matched literature data on the shear modulus obtained by rheometry.

In this study, we performed 1-to-1 comparison of corneal moduli measured with AμT-OCE with 2 mechanical tests (parallel plate rheometry and tensile extensometry) performed on the same corneal samples. Nine fresh porcine corneas were measured to limit individual variations in the cornea's mechanical properties. Although this study demonstrated markedly different corneal stiffness under shear versus tensile loading, some differences exist between AμT-OCE and destructive mechanical testing methods that can make direct comparisons difficult. Indeed, effects such as corneal curvature, its nonlinearity, boundary conditions in mechanical loading, loading direction, engineering strain, hydration, preconditioning, and others can influence moduli estimates in mechanical tests. Estimates provided by AμT-OCE should be more accurate representations of in vivo biomechanics because this noncontact and noninvasive measurement procedure was performed under well-controlled IOP. A key takeaway from this study is that moduli quantified from OCE data analyzed with the NITI model can be generalized across different systems.

In extension loading, corneal shape is different from inflation. The cornea preserved its curvature in OCE measurements, whereas the curvature was flattened in tensile testing. Axial extension, which causes the cornea to flatten, induces compressional forces and produces different strain distributions for cornea under inflation versus extension.

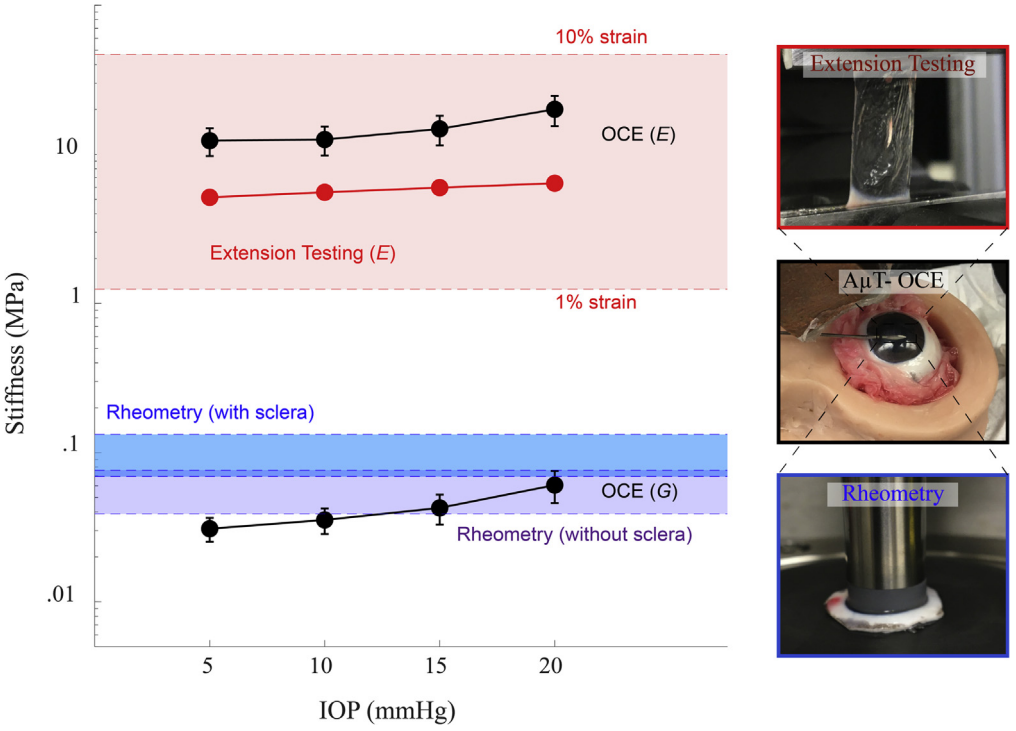

Figure 2. Moduli (*E*, assuming tensile isotropy, and G) estimates from acoustic microtapping OCT elastography (AμT-OCE; black), parallel-plate rheometry (blue), and strip extension (red). The red box denotes the range of elastic moduli measured at strains of 1% to 10% and the red dots denote the equivalent strain estimate at intraocular pressures (IOPs) representative of in vivo conditions (detailed in Supplemental Methods). The darker blue box is the storage shear modulus (G′) measured via rheometry with the scleral ring attached, and the purple box corresponds to values appropriately scaled to account for the apparent stiffness from inclusion of the scleral ring (detailed in Supplemental Methods).

Additionally, the cornea was under biaxial tension in OCE and uniaxial tension in extension. The force is assumed to be equally distributed across the cornea considering a true cuboid shape (uniform thickness and cross-section). However, the central cornea thickness is thinner than the periphery and exhibits varied radius along the center line compared with the edge of the strip, complicating interpretation of results.[11] Corneal samples were not uniform thickness, suggesting that the axial strain at the center of the sample may differ from that at the perimeter during loading. This effect was not adjusted for in this analysis. Nevertheless, our measurements of Young's modulus acquired from both AμT-OCE and extension testing are consistent with those in porcine cornea strips subject to tensile loading (0.3−29 MPa[12−18]).

The order of magnitude difference in the modulus measured under shear loading was higher than previously reported values of *G* (0.3−9 kPa[19−21]). Because corneal buttons were loaded in unconfined compression, tissue at the corneal−scleral junction splayed outward beyond the probe. Rheometry was performed on an independent set of corneas both with and without the scleral rim attached (Supplemental Methods). The remaining tissue was shown to produce an approximately 2-fold increase in the measured modulus. This suggests that the tissue splayed beyond the probe provides additional resistance to shearing, overestimating the corneal modulus. Additionally, the corneoscleral boundary may contribute to residual stress within the cornea compared with the corneal button alone.[22] The shear modulus of the cornea has been shown to increase with higher compressional preload,[19] suggesting that internal forces resulting from both parallel-plate rheometry and increased residual stress may increase the measured transverse shear modulus. The hypothesis that residual stress within whole-globe samples may contribute to a higher transverse shear modulus likely warrants further study and may describe the discrepancy between the values measured via OCE and those reported in the literature.

Internal pressures estimated in the cornea resulting from flattening during tonometry do not seem to induce large structural changes within the tissue at low IOP, suggesting that flattening alone will have a small effect on the shear modulus.[23] In this case, flattening resulting from the parallel-plate arrangement was assumed to have a small effect on the measured modulus. However, it should be noted that during rheometry, tissue at the center undergoes a smaller shear strain than that at the outer edge. The center of the tissue also may experience different compressive strain resulting from corneal thinning, an effect that was ignored in this study. Additionally, the frequency range used by OCE differed from that of rheometry. Although OCE functionally measures higher-frequency vibrations (range, 0.3−4 kHz), the relatively lower frequency (multiple hertz range) probed in rheometry suggests that frequency-dependent differences likely exist between the moduli measured by the 2 methods.

Direct mechanical tests performed in this study with different loading methods confirm corneal mechanical anisotropy. A difference of at least 1 order of magnitude in elastic moduli determined from tensile tests compared with rheometry on the same corneas (see Fig 2) cannot be described with the same modulus. The simplest assumption accounting for such difference is corneal transverse isotropy. Indeed, the elastic properties of collagen fibers have been shown to differ from those of corneal connective tissue,[24–26] suggesting that the preferred collagen orientation results in asymmetric elastic properties. The NITI model used in this study to reconstruct mechanical moduli from AμT-OCE produces estimates of both elastic moduli, μ and G, which are in good agreement with moduli obtained with mechanical tests. However, as noted in the Supplemental Methods, the NITI model is simplified by assuming corneal tensile isotropy, that is, isotropic Young's modulus (E), although tensile and shear deformations are driven by different moduli.

To account for tensile anisotropy, an additional parameter δ should be introduced. Supplemental Figure 3 (see Supplemental Methods) shows the level of the Young's modulus anisotropy allowed by corneal symmetry, with the in-plane Young's modulus possibly varying between 2μ (for the strongest tensile anisotropy) and 3μ (for tensile isotropy). Determining the parameter δ is not easy and is the subject of our future studies. In this study, we used $\delta = 0$, and therefore Young's modulus $E = 3\mu$. The comparison between tensile and AμT-OCE measurements for E suggests that its OCE-based value may be overestimated. If the relationship $E = 2\mu$ (corresponding to $\delta = -2\mu$) had been used, both methods would have demonstrated very close agreement. Thus, the in-plane Young's modulus of cornea is likely closer to its lower limit, rather than to its highest possible value, as presented here. However, additional studies should be performed to confirm this observation. Nevertheless, we emphasize that using a simplified NITI material model rather than a simple isotropic model is an important step in quantifying anisotropic properties in the cornea because it separates the effects of μ from G, which are much greater than any possible variations of E introduced by $\delta \neq 0$.

Young's and shear moduli were assumed to be nonvarying in depth. Quantifying depth-dependent moduli in the cornea likely will require complex models of high frequency content or additional loading techniques. Viscous effects also were not included in this study. Recent models incorporating viscosity suggest a second-order effect in the frequency range of mechanical waves considered in this study. To account for viscosity, higher-frequency components of propagating elastic waves[27] should be considered. This represents another direction to improve quantitation of corneal viscoelasticity.

This study suggests that robust and accurate measurements of corneal elastic moduli can be achieved using noncontact AμT-OCE. Although in-plane anisotropy (within the xy-plane) has been reported in some studies, the degree of anisotropy remains low at low IOP.[16,28–31] This suggests that for normal IOPs (less than 25 mmHg in porcine cornea), corneal microstructure can be approximated with the NITI model (i.e., symmetric for any direction in the xy-plane).

It also should be noted that significant effort has been directed toward personalized biomechanical models suitable for screening, surgical planning, and treatment monitoring. Because corneal mechanical properties determine its shape, it is important that accurate moduli are input to biomechanical models to predict static deformation and shape.[32] Although such static models remain largely in the development stage, advanced models assuming a transverse isotropic tissue structure seem most robust.[33,34]

Because AμT-OCE seem to quantify mechanical properties in the cornea accurately, whereas OCT can image its structure and shape simultaneously, an OCT-based technique is a very promising direction to develop personalized biomechanical models. Such personalized models potentially can be used to study disease progression and may play a role in treatment based on simulated interventions. Future studies to assess anisotropy in diseased cornea may improve our understanding of pathologies further and potentially may inform treatment. Additional studies using faster OCT imaging systems capable of B-M scanning (where a single acoustic push is tracked using repeated B-scans), as well as higher resolution OCE reconstruction methods, may increase the usefulness of AμT-OCE in the clinic. Assuming that in vivo OCE methods can measure moduli robustly and reliably, it is likely that truly noncontact methods will pave the way for clinical translation.

Acknowledgments

The authors thank Dr. Yak-Nam Wang and the Center for Industrial and Medical Ultrasound at the University of Washington for their assistance in acquiring tissue samples and Kit Hendrickson for figure illustrations.

Footnotes and Disclosures

Originally received: May 25, 2021.
Final revision: September 14, 2021.
Accepted: September 15, 2021.
Available online: September 22, 2021. Manuscript no. D-21-00090.

[1] Department of Bioengineering, University of Washington, Seattle, Washington.

[2] Department of Ophthalmology, University of Washington, Seattle, Washington.

Disclosure(s):

All authors have completed and submitted the ICMJE disclosures form.

The author(s) have made the following disclosure(s): R.W.: Consultant – Carl Zeiss Meditec, Inc.

Supported in part by the National Institutes of Health, Bethesda, Maryland (grant nos.: R01-EY026532, R01-EY024158, R01-EB016034, R01-CA170734, R01-AR077560, and R01-HL093140); Life Sciences Discovery Fund (no.: 3292512); the Coulter Translational Research Partnership

Program; Research to Prevent Blindness, Inc., New York, New York (unrestricted grant); the Department of Bioengineering, University of Washington, Seattle, Washington; and the National Science Foundation (graduate fellowship no.: DGE-1256082 [M.A.K.]). This material was based on work supported by the National Science Foundation Graduate Research Fellowship Program (grant no.: DGE-1256082).

The authors declare that all data from this study are available within the article and its supplemental material. Raw data for the individual measurements are available on reasonable request.

HUMAN SUBJECTS: No human subjects were included in this study.

Nonhuman animals were used in this study. No patient-level consent or institutional review board approval were required. All research adhered to the tenets of the Declaration of Helsinki.

Author Contributions:

Conception and design: Kirby, Pelivanov, O'Donnell, Shen

Analysis and interpretation: Kirby, Liou, Pelivanov, O'Donnell, Shen

Data collection: Kirby, Pitre, Li, Shen

Obtained funding: Wang, O'Donnell, Shen

Overall responsibility: Kirby, Pitre, Liou, Li, Wang, Pelivanov, O'Donnell, Shen

Abbreviations and Acronyms:
AμT = acoustic microtapping; **BSS** = balanced saline solution; **IOP** = intraocular pressure; **NITI** = nearly incompressible transversely isotropic; **OCE** = OCT elastography.

Keywords:
Cornea, Elastic anisotropy, NITI model, OCT elastography, Young's modulus.

Correspondence:
Tueng T. Shen, MD, PhD, Department of Bioengineering, University of Washington, 3720 15th Ave NE, Seattle, WA 98105. E-mail: ttshen@uw.edu.

References

1. Gandhi S, Jain S. The anatomy and physiology of cornea. *Keratoprostheses Artif Corneas Fundam Surg Appl*. 2015;37:19–25.
2. Meek KM, Knupp C. Corneal structure and transparency. *Prog Retin Eye Res*. 2015;49:1–16.
3. De Moraes C. Risk factors for visual field progression in treated glaucoma. *Arch Ophthalmol*. 2011;129:562–568.
4. Roberts C. Concepts and misconceptions in corneal biomechanics. *J Cataract Refract Surg*. 2014;40:862–869.
5. Kirby MA, Pelivanov I, Song S, et al. Optical coherence elastography in ophthalmology. *J Biomed Opt*. 2017;22:1–28.
6. Pitre JJ, Kirby MA, Li DS, et al. Nearly-incompressible transverse isotropy (NITI) of cornea elasticity: model and experiments with acoustic micro-tapping OCE. *Sci Rep*. 2020;10:12983.
7. Faber C, Scherfig E, Prause JU, Sørensen KE. Corneal thickness in pigs measured by ultrasound pachymetry in vivo. *Scand J Lab Anim Sci*. 2008;35:39–43.
8. Lin RC, Shure MA, Rollins AM, et al. Group index of the human cornea at 13-μm wavelength obtained in vitro by optical coherence domain reflectometry. *Opt Lett*. 2004;29:83.
9. Fratzl P. *Collagen: structure and mechanics, an introduction*. Boston, MA: Springer; 2008:1–13.
10. Girard MJA, Dupps WJ, Baskaran M, et al. Translating ocular biomechanics into clinical practice: current state and future prospects. *Curr Eye Res*. 2015;40:1–18.
11. Khan MA, Elsheikh A, Rizvi ZH, Ahmad Khan I. Influence of analytical methods versus clamping procedure on biomechanical response of cornea through experimental strip tests. *Mater Today Proc*. 2021;44:4375–4380.
12. Bekesi N, Dorronsoro C, De La Hoz A, Marcos S. Material properties from air puff corneal deformation by numerical simulations on model corneas. *PLoS One*. 2016;11:e0165669.
13. Boschetti F, Triacca V, Spinelli L, Pandolfi A. Mechanical characterization of porcine corneas. *J Biomech Eng*. 2012;134:031003.
14. Wollensak G, Spoerl E, Seiler T. Stress-strain measurements of human and porcine corneas after riboflavin-ultraviolet-A-induced cross-linking. *J Cataract Refract Surg*. 2003;29:1780–1785.
15. Zeng Y, Yang J, Huang K, et al. A comparison of biomechanical properties between human and porcine cornea. *J Biomech*. 2001;34:533–537.
16. Elsheikh A, Alhasso D. Mechanical anisotropy of porcine cornea and correlation with stromal microstructure. *Exp Eye Res*. 2009;88:1084–1091.
17. Hatami-Marbini H, Jayaram SM. Effect of UVA/riboflavin collagen crosslinking on biomechanics of artificially swollen corneas. *Invest Ophthalmol Vis Sci*. 2017;59:764–770.
18. Lanchares E, Del Buey MA, Cristóbal JA, et al. Biomechanical property analysis after corneal collagen cross-linking in relation to ultraviolet A irradiation time. *Graefes Arch Clin Exp Ophthalmol*. 2011;249:1223–1227.
19. Hatami-Marbini H. Viscoelastic shear properties of the corneal stroma. *J Biomech*. 2014;47:723–728.
20. Aslanides IM, Dessi C, Georgoudis P, et al. Assessment of UVA-riboflavin corneal cross-linking using small amplitude oscillatory shear measurements. *Invest Ophthalmol Vis Sci*. 2016;57:2240–2245.
21. Søndergaard AP, Ivarsen A, Hjortdal J. Corneal resistance to shear force after UVA-riboflavin cross-linking. *Invest Ophthalmol Vis Sci*. 2013;54:5059–5069.
22. Lanir Y. Mechanisms of residual stress in soft tissues. *J Biomech Eng*. 2009;131:1–5.
23. Racia AR, Urita JZ, In DPP. Automatized patient-specific methodology for numerical determination of biomechanical corneal response. 2016;44:1753–1772.
24. Boote C, Dennis S, Huang Y, et al. Lamellar orientation in human cornea in relation to mechanical properties. *J Struct Biol*. 2005;149:1–6.
25. Anderson K, El-Sheikh A, Newson T. Application of structural analysis to the mechanical behaviour of the cornea. *J R Soc Interface*. 2004;1:3–15.
26. Thomasy SM, Raghunathan VK, Winkler M, et al. Elastic modulus and collagen organization of the rabbit cornea: epithelium to endothelium. *Acta Biomater*. 2014;10:785–791.
27. Ramier A, Tavakol B, Yun S-H. Measuring mechanical wave speed, dispersion, and viscoelastic modulus of the cornea using optical coherence elastography. *Opt Express*. 2019;27:16635.
28. Ambroziński Ł, Song S, Yoon SJ, et al. Acoustic microtapping for non-contact 4D imaging of tissue elasticity. *Sci Rep*. 2016;6:38967.
29. Nguyen TD, Boyce BL. An inverse finite element method for determining the anisotropic properties of the cornea. *Biomech Model Mechanobiol*. 2011;10:323–337.

30. Li J, et al. Revealing anisotropic properties of cornea at different intraocular pressures using optical coherence elastography. *Opt Elastography Tissue Biomech III*. 2016;9710: 97100T.
31. Singh M, Li J, Han Z, et al. Investigating elastic anisotropy of the porcine cornea as a function of intraocular pressure with optical coherence elastography. *J Refract Surg*. 2016;32:562−567.
32. Schachar RA, Abolmaali A. Proper material properties are required for the finite element method. *Arch Ophthalmol*. 2006;124:1064−1065.
33. Wang S, Hatami-Marbini H. Constitutive modelling of cornea tissue; influence of three-dimensional collagen fiber microstructure. *J Biomech Eng*. 2021;143:031002.
34. Pandolfi A. Cornea modelling. *Eye Vis*. 2020;7:1−15.